Optical and chemical sensor properties of Langmuir-Blodgett thin films coated with N-cyclohexylmethacrylamide monomer

M. ERDOGAN[a], Y. ACIKBAS[b,*], C. SOYKAN[b], N. CANKAYA[c], R. CAPAN[a]
[a]*Department of Physics, Faculty of Science, University of Balikesir, Turkey*
[b]*Department of Material Science and Nanotechnology Engineering, Faculty of Engineering, University of Usak, Turkey*
[c]*Department of Chemistry, Faculty of Science, University of Usak, Turkey*

In this work, N-cyclohexylmethacrylamide (NCMA) Langmuir-Blodgett (LB) thin films are characterized by Surface Plasmon Resonance (SPR) and Quartz Crystal Microbalance (QCM). The fitted SPR data is utilized to be calculating the film thickness of this material and is found to be as 0.76±0.08 nm for single layer. The sensing behaviors of LB films are investigated with respect to volatile organic compounds (VOCs) at room temperature. The sensing responses of the films against to VOCs are measured by the QCM method. It is found that the NCMA film exhibits good response, reversibility, stability, fast response and recovery characteristic to VOCs.

(Received April 24, 2018; accepted October 10, 2018)

Keywords: Monomer, LB thin film, Vapor sensor, Quartz crystal microbalance, Surface plasmon resonance

1. Introduction

Polymers and their derivatives have been attracting the attention and interest of researchers in many fields because of their remarkable properties leading to potential applications in biology [1,2], life sciences [3,4], drug delivery systems [5,6], tissue engineering [7], solar cells [8,9], optical devices [10], organic electronic materials [11], organic photovoltaic devices [12] and chemical sensors [13]. For the development of chemical sensors (devices for detecting gases and volatile organic compounds (VOCs)), these materials promise reduced cost, higher portability and operation at low power and as a result have actually received considerable attention. The preparation of polymeric materials with ordered nanostructures has attracted an increasing interest in recent years and various techniques of thin film fabrication have been explored [14-16]. In particular, LB technique can offer an effective way to prepare the well defined structures of polymeric film, since thickness and molecular orientation of the produced LB film can be easily controlled, compared with other coating methods. There are many studies about the monolayer behaviors of the polymer compounds at the air-water interface [17,18], which are investigated with their corresponding Π-A isotherms, and the fabrication of LB thin film onto solid substrate such as glass, quartz glass and quartz crystal [19,20].

In recent years, research and development of vapor sensing systems using several measurement techniques, such as SPR, UV-visible and QCM, have been carried out by many researchers [21-23]. Among them, QCM is a measurement technique that has a low-cost, and being based on piezoelectric effect is appropriate for gravimetric VOC sensors. The frequency of QCM resonator (quartz crystal) decreases with mass loading due to the VOCs vapor aggregation on quartz crystal's surface, which is coated with a chemo-selective layer [24,25]. It is considered that the change of frequency is a sensor signal for the VOCs vapor recognition.

In the present work, NCMA material is used to investigate LB thin film characterization and sensing properties against the following organic vapors: chloroform ($CHCl_3$), dichloromethane (CH_2Cl_2), benzene (C_6H_6) and toluene (C_6H_5-CH_3). This study shows that NCMA monolayer has a very uniform arrangement at the air-water interface and they are transferred as LB layers onto the quartz crystal and gold-coated glass substrates. The thin film characterization of these layers is monitored by SPR technique. The vapor sensing measurements are carried out using the QCM system. This material shows very promising results in the field of room temperature vapor sensors with a fast, large and reproducible response to dichloromethane vapor.

2. Experimental details

2.1. LB film preparation

The synthesis of the NCMA monomer is shown in Fig. 1 and detailed synthesis process of this material is given in our previous study [26]. Alternate layer Nima 622 model LB film trough provided with a filter paper Wilhemly balance was employed to record the surface pressure–area (Π-A) which is called as isotherm graphs and to fabricate the thin films. A Lauda Ecoline RE204 model temperature control unit was connected to the LB

trough to control the temperature of the water subphase. All measurements were carried out at room temperature. NCMA was dissolved in chloroform with a concentration of 0.22 mg ml^{-1}. The different volumes of solution were spread onto the pure water subphase using a Hamilton syringe allowing approximately 15 min for the solvent to evaporate. After this procedure, the Π-A isotherm of NCMA was recorded with the compression speed of 30 cm^2 min^{-1}. The isotherm graph was taken several times and was found to be reproducible. Π-A graph was used to select the surface pressure value. Monolayer was transferred at the constant surface pressure value of 18 mN m^{-1} onto gold-coated glass substrates for SPR measurement and onto quartz substrates for QCM measurement by the vertical dipping method [26].

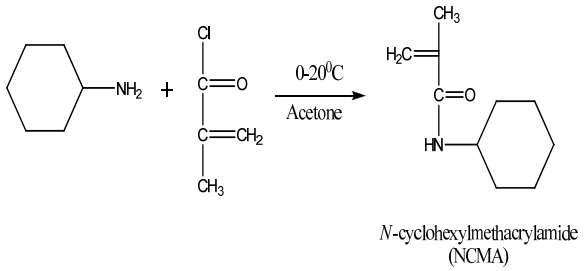

Fig. 1. Synthesis of the NCMA monomer

2.2. SPR and QCM measurement systems

Surface Plasmon Resonance Spectrometer (BIOSUPLAR 6Model) with a low power laser diode (630–670 nm) light source was employed to perform SPR measurements with an angular resolution of 0.003°. A glass prism (n = 1.62) is mounted within a holder so as to be available for measurement in liquid or in air environments. Glass slides with the dimensions 20mm×20mm×1mm are coated on top by a very thin homogeneous layer of gold. A transparent plastic flow cell was made in house to be allowing vapor measurements. The cell has two channels, with inlets and outlets connected to silicone tubes. Biosuplar-Software was used to control the SPR system settings, measurements and data acquisition as well as data presentation. Several modes such as single measurements, tracking mode or slope mode can be utilized and the signal displayed as a function of time. Variations within both measurement channels can be displayed in real time using this software. The photodetector response was monitored as a function of time during periodic exposure of the sample to the organic vapor for at least 2 minutes, this was then allowed to recover after injection of dry air. WINSPALL software developed at the Max-Plank-Institute for Polymer Research, Germany was utilized for the fitting of SPR curves to determine thickness values of the LB films.

In order to study the sensing properties of NCMA LB film, a thinly cut wafer of raw quartz sandwiched between two electrodes in an overlapping keyhole design was used for the QCM measurement. A block diagram of our home made QCM measurement system is shown in Fig. 2. Standard QCM crystals with a nominal resonance frequency of 3.5 MHz were commercialized from GTE SYLVANIA company. All experiments were carried out at room temperature using an oscillating circuit designed by us. The quartz crystal was inserted into the electronic control unit, and the frequency of oscillation was monitored as a function of time using dedicated software. The values of frequency changes, which indicate the degree of response, are measured with an accuracy of 1 Hz. After each deposition cycle, the LB film sample was dried for half an hour and the mass change was monitored using this computer controlled QCM measurement system. This system was used for the confirmation of the reproducibility of LB film multilayers using the relationship between the QCM frequency changes against the deposited mass, which should depend on the number of layers in the LB film.

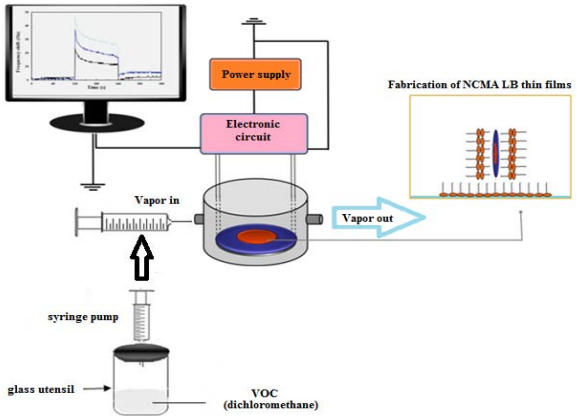

Fig. 2. A block diagram of the quartz crystal microbalance measurement system

A gas cell was constructed to study the LB film response on exposure to organic vapors by measuring the frequency change and these measurements were performed with a syringe. The sample was periodically exposed to organic vapors at least for 2 minutes, and was then allowed to recover after injection of dry air. The changes in resonance frequency were recorded in real time during exposure to organic vapors. The exposure to VOC vapor for 2 minutes was followed by flushing of the cell with dry air for another 2 minutes. This procedure was carried out over several cycles to observe the reproducibility of the LB film sensing element.

3. Results and discussion

3.1. SPR results

Fig. 3 shows a shematic diagram of Kretschmann configuration for optical measurement system of prism-gold layer-LB thin film layer of NCMA molecules-air. SPR is an optical detection process that occurs when a p-polarized monochromatic He-Ne laser light (λ= 632.8 nm)

hits a prism covered by NCMA LB film layer onto the gold-coated slide substrate. An optical contact between these samples and prism (of refractive index n_p= 1.515) was made using an index matching liquid (ethylsalicylate from Aldrich). Under certain conditions (wavelength, polarization and incidence angle) free electrons at the surface of the gold layer absorb incident light photons and convert them into surface plasmon waves. At a specific incidence angle, which is known SPR angle, the plasmon waves resonate with the incident light, resulting in a dip of reflectivity.

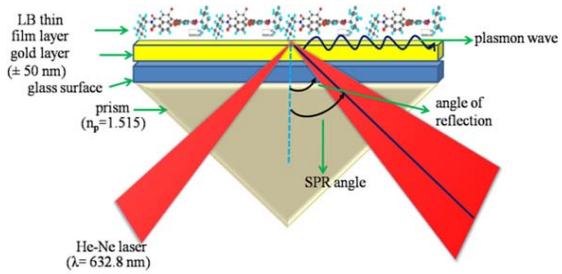

Fig. 3. A shematic diagram of Kretschmann configuration for optical measurement system of prism-gold layer-LB thin film layer of NCMA molecules-air

SPR measurements were made on the LB films deposited onto gold-coated glass substrates with Y-type deposition at a lateral pressure of 18 mN m^{-1}. Fig. 4 shows a set of experimental SPR curves showing the variation of reflected intensity as a function of internal angle for NCMA LB films. The SPR curve of the bare gold was also used as a reference. The SPR curves of NCMA LB films of four different thicknesses are shifted to larger angles when the number of layers is increased. The inset in Fig. 4 displays the peak shifts (Δθ) seen in the angular scans of the plasmon resonance curves of the LB film multilayer assemblies relative to bare gold, increased linearly with the number of layers. A linear relationship suggests that equal mass per unit area is deposited onto the gold-coated glass substrate during the transfer of LB film layers.

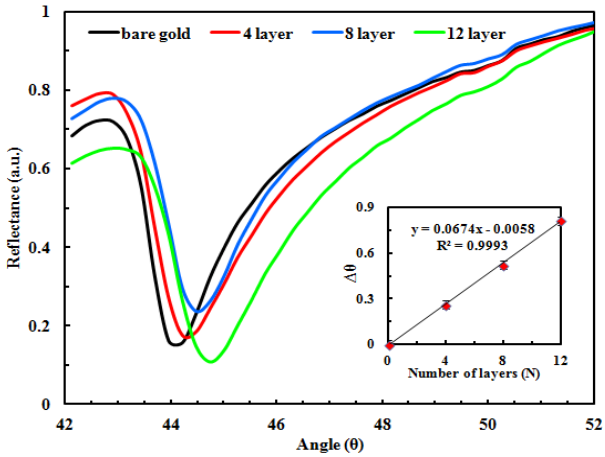

Fig. 4. SPR curves of NCMA LB films with increase in thickness. Inset: linear increase of thickness as a function of number of bilayers

3.2. Calculation of thickness of NCMA LB film

The experimental SPR data were fitted using the Winspall software (written by Wolfgang Knoll, developed at the Max-Plank- Institute for Polymer Research, Germany) [27] in order to evaluate the film thickness (d). It was assumed that the extinction coefficent, *k* is zero for our LB films, since they are transparent at λ=633 nm [28]. Fig. 5 presents the experimentally measured and theoretically fitted SPR curves for the uncoated gold film and for the same gold film coated with 8 monolayers of NCMA. Similar calculations carried out for 4, 8 and 12 layers and the fitting calculations produce a mean value of 0.76±0.08 nm for the thickness per monolayer. Fig. 6 shows that the thickness of NCMA LB films increases linearly with the number of layers, as expected for this system.

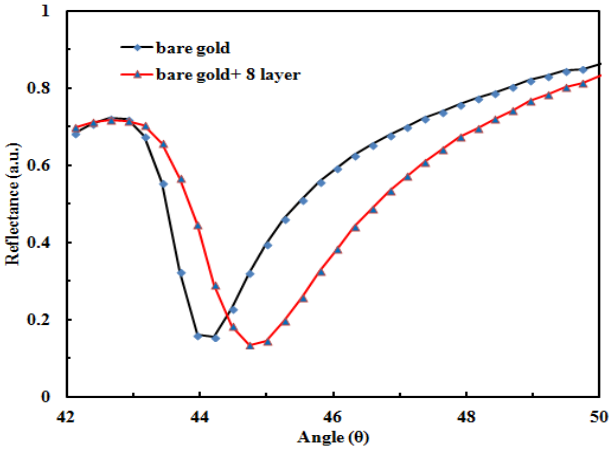

Fig. 5. Complete measured (dots) and fitted (lines) SPR curves for clean gold surface and 8 layer NCMA LB film

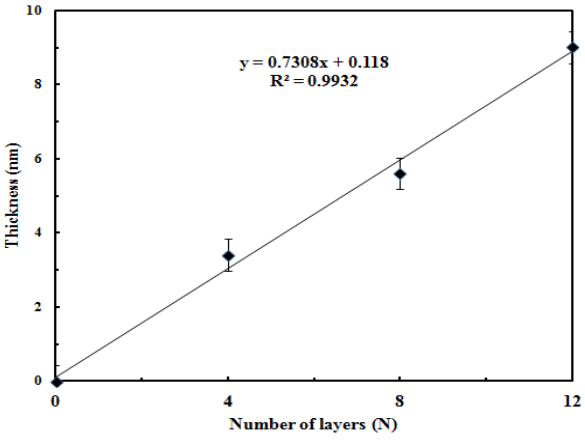

Fig. 6. Modeled layer thickness as a function of layer number for NCMA LB layers. The solid line is a linear regression fit to the data (R^2 = 0.9932)

3.3. Swelling properties of NCMA LB film

The kinetic responses of all 12 layered NCMA LB thin films investigated using QCM technique in terms of

the change in resonance frequency (Δf). It is clearly seen that the relatively high values obtained for chlorinated aliphatic hydrocarbons especially for dichloromethane is noteworthy. The NCMA LB film is periodically exposed to the organic vapors for 2 minutes, followed by the injection of dry air for a further 2 minutes period. Fig. 7 shows the kinetic response of NCMA LB film to dichloromethane, chloroform, benzene and toluene vapors by using QCM measurement system.

In the initial step, the monomer LB film sensor expose to dry air for 120 seconds and the response was a stable value in this period of time. The initial response of monomer LB film in the QCM system for all vapors increased sharply between 120 and 125 s due to surface adsorption effect. When the vapor molecules moved into the monomer LB film sensor, the response decreased exponentially due to the bulk diffusion effect. In the 240 s, after flushing dry air, a rapid decrease of response was observed and then recovery process occured between 240 and 244 s for all vapors due to desorption of organic vapor. After 245 s, the response of monomer LB film sensor reached a stable value and the sensor obtained initial baseline. As seen in Fig. 7, the response of the LB thin film to these organic vapors is fast, reproducible and reversible. As a result, it can be considered that kinetic response mechanism occurs by a 3-stage (adsorption, diffusion, and desorption processes, respectively).

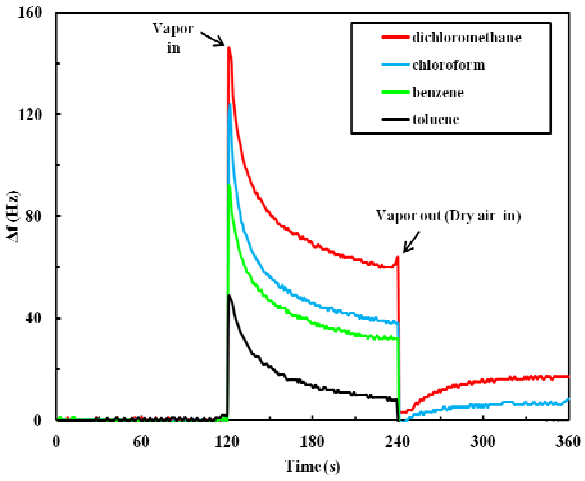

Fig. 7. The frequency change of NCMA LB film against organic vapors

When Fick's second law of diffusion is applied to a plane sheet and solved by assuming a constant diffusion coefficient, the following equation is obtained for concentration changes in time: [29]

$$\frac{C}{C_0}=\frac{x}{d}+\frac{2}{\pi}\sum_{n=1}^{\infty}\frac{\cos n\pi}{n}\sin\frac{n\pi x}{d}\exp(-\frac{Dn^2\pi^2}{d^2}t) \quad (1)$$

where d is the thickness of the slab, D is the diffusion coefficient, and C_0 and C are the concentration of the diffusant at time zero and t, respectively. x corresponds to the distance at which C is measured. We can replace the concentration terms directly with the amount of diffusant by using:

$$M=\int_V CdV \quad (2)$$

where M is the mass uptake and V is the volume element. When Eq. 1 is considered for a plane volume element and substituted in Eq. 2, the following solution is obtained [30].

$$\frac{M_t}{M_\infty}=1-\frac{8}{\pi^2}\sum_{n=0}^{\infty}\frac{1}{(2n+1)^2}\exp(-\frac{(2n+1)^2D\pi^2}{d^2}t) \quad (3)$$

where M_t penetrant mass sorbed into the deposited film, assuming a one-dimensional geometry. The quantity, M_∞, represents the amount sorbed at equilibrium, t is the time. This equation can be reduced to a simplified form:

$$\frac{M_t}{M_\infty}=4\sqrt{\frac{D}{\pi d^2}t^{1/2}} \quad (4)$$

which is called early-time equation and this square root relation can be used to interpret the swelling data [31,32].

In order to measure the kinetic data given in Fig. 7 it is required to take the monomer LB film parameters due to swelling process. Fig. 8 represents the normalized frequency change against swelling time where the consolidation process involves setting starting times to $t=0$ for each swelling cycles. As seen in Fig. 8, the normalized frequency decreased as the time of vapor exposure increased. It is also seen that changes in the normalized frequency against the time of vapor exposure decreased very fast as the dichloromethane saturated concentration injected into the gas cell is increased. These behaviors can be declared with the chain inter diffusion between monomer chains during vapor exposure. As the saturated dichloromethane vapors penetrate into monomeric film, the monomer chains interdiffuse, which results in the decrease of the normalized frequency from the monomeric film. These results can be related to the amounts of diffusant entering the monomeric film M_t; that is, Δf_t should be directly proportional to M_t [29,33]. Eq. 4 now can be written as:

$$\left(\frac{M_t}{M_\infty}\right):\left(\frac{\Delta f_t}{\Delta f_\infty}\right)=4\sqrt{\frac{D}{\pi d^2}t^{1/2}} \quad (5)$$

where Δf_t and Δf_∞ are the normalized frequency shift at any time, t and saturation point in Δf, respectively. The

normalized Δf values [$\Delta f_t / \Delta f_\infty$] are plotted in Fig. 9 for the square root of swelling time according to Eq. 5. The slopes of the linear relations in Fig. 9 found the diffusion coefficients, *D* for the swelling of monomeric film and those values are found as 7.02 x10^{-16}, 3.92 x10^{-16}, 2.72 x10^{-16} and 1.55 x10^{-16} cm^2s^{-1} for dichloromethane, chloroform, benzene and toluene, respectively.

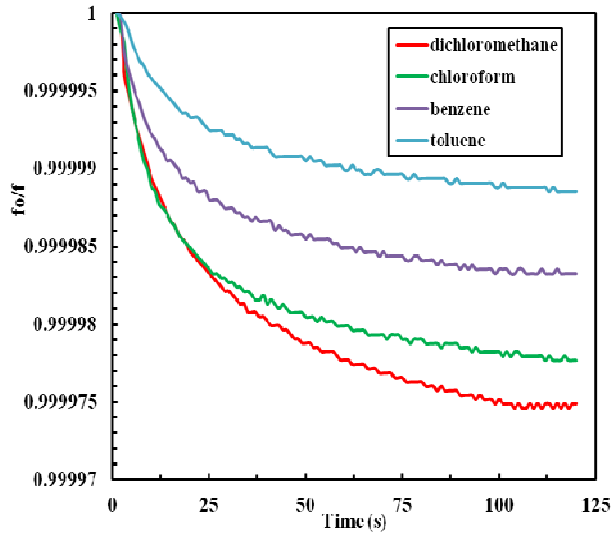

Fig. 8. Normalized frequency changes against swelling time, t_s for organic vapors

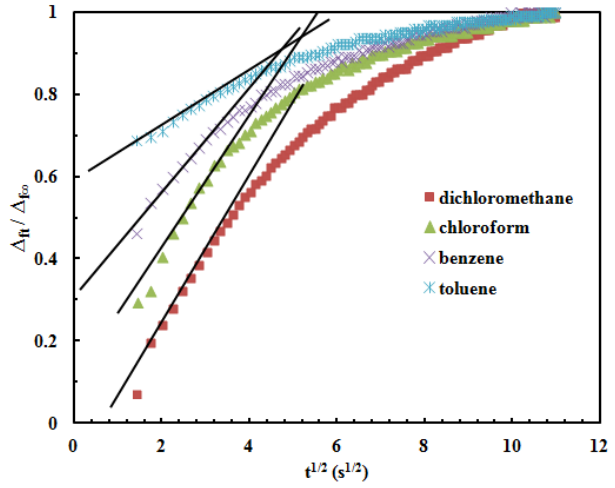

Fig. 9. Plot of the normalized frequency against square root of swelling time. The solid line represents the fit of the data to Eq. (5).

These results can be explained in terms of molar volume of organic vapors. VOCs molecules enter into the monolayer chains and expand the volume of chain causing swelling. The interaction of produced NCMA thin films with VOCs molecules depended on physical properties of organic vapors such as molar volume and viscosity. The values of molar volume are known as dichloromethane (64.10 cm^3 mol^{-1}) < chloroform (80.70 cm^3 mol^{-1}) < benzene (86.36 cm^3 mol^{-1}) < toluene (107.00 cm^3 mol^{-1}). While dichloromethane molecule can easily penetrate into NCMA LB films, the diffusion of the other organic vapor molecules into the same LB films is slower. Similar relationship can also be observed with the effect of viscosity. The viscosity values of dichloromethane and chloroform vapors (0.324 and 0.380 cSt) are higher than the toluene and benzene (0.680 and 0.744 cSt) vapors, respectively. Dichloromethane molecule can easily penetrate into NCMA LB films since it has the lowest value of viscosity among organic vapors used in this work. It is possible to find similar studies in the literature investigating VOCs sensing properties of polymer molecules [34,35]. In our previous study poly[(Styrene (ST)-co-Glycidyl Methacrylate (GMA)] copolymer LB thin film sensor materials were exposed to dichloromethane, chloroform, benzene, toluene and ethanol vapors and the copolymer LB films were obtain to be largely sensitive to dichloromethane vapor [34]. The poly(3-hexylthiophene) (P3HT) and poly(3-dodecylthiophene) (P3DT) materials were used as sensor materials for the optical detection of VOCs using UV-vis spectroscopy (transmission mode). Both polymers were tested with five VOCs (dichloromethane, chloroform, n-hexane, THF and toluene) [35]. Although the detection techniques used are different, chemical sensors show the largest sensitivity against dichloromethane vapor.

4. Conclusion

In this study, NCMA monomer was characterized and its gas sensing properties were investigated using SPR and QCM techniques. The fitted SPR data was used to be calculating the film thickness of NCMA material. The fitting calculations produced a mean value of 0.76±0.08 nm for the thickness per monolayer and the thickness of NCMA LB films increases linearly with the number of layers. Vapor sensing properties of these LB films against four volatile organic compounds (VOCs) dichloromethane, chloroform, benzene and toluen were studied using the QCM technique. NCMA LB film was exposed to dichloromethane, chloroform, benzene and toluene vapors. It was shown that the penetration of organic vapors into NCMA LB film is quick enough and diffusion coefficients are connected on the VOCs used. This result can be related in terms of molar volume of swelling items. Diffusion coefficients found to be 7.02 x10^{-16}, 3.92 x10^{-16}, 2.72 x10^{-16} and 1.55 x10^{-16} cm^2s^{-1} for dichloromethane, chloroform, benzene and toluene vapors, respectively. Diffusion coefficients for dichloromethane are higher than other organic vapors because dichloromethane has lowest molar volume parameter which indicates that dichloromethane molecules are more mobile than the other organic vapors and diffuse easily into the NCMA LB film. Otherwise, toluene has a larger molar volume parameter which means these molecules are slow to diffuse into the NCMA LB film, indicating lower diffusion coefficients than other organic vapors used in this work. As a result, this NCMA material can be used as a sensing material and may find

potential applications in the development of room temperature organic vapor sensing devices.

Acknowledgements

The authors would like to thank The Research Foundation of Usak University (BAP) for financial support of this work. Project no.: 2014/MF014.

References

[1] E. B. Anderson, T. E. Long, Polymer **51**, 2447 (2010).
[2] L. Rocha, C. M. Paius, A. L. Raicu, E. Resmerita, A. Rusu, I. A. Moleavin, M. Hamel, N. Branza-Nichita, N. Hurduc, J. Photoch. Photobio. A **291**, 16 (2014).
[3] M. C. Celina, Polym. Degrad. Stabil. **98**, 2419 (2013).
[4] D. Vasiukov, S. Panier, A. Hachemi, Int. J. Fatigue **70**, 289 (2015).
[5] A. Sosnik, J. Neves, B. Sarmento, Prog. Polym. Sci. **39**, 2030 (2014).
[6] O. Sedláček, J. Kučka, M. Hrubý, Appl. Radiat. Isotopes **95**, 129 (2015).
[7] T. H. Qazi, R. Rai, A. R. Boccaccini, Biomaterials **35**, 9068 (2014).
[8] U. J. Lee, S. H. Lee, J. J. Yoon, S. J. Oh, S. H. Lee, J. K. Lee, Sol. Energ. Mat. Sol. C, 108 (2013).
[9] M. L. Cantu, A. Chafiq, J. Faissat, I. G. Valls, Y. Yu, Sol. Energ. Mat. Sol. C **95**, 1362 (2011).
[10] N. A. M. Yahya, W. H. Lim, K. D. Dambul, S. W. Phang, H. Ahmad, R. Zakaria, F. R. Mahamd Adikan, Opt. Mater. **34**, 1735 (2012).
[11] A. Bousquet, H. Awada, R. C. Hiorns, C. D. Lartigau, L. Billon, Prog. Polym. Sci. **39**, 1847 (2014)
[12] N. P. Holmes, S. Ulum, P. Sista, K. B. Burke, M. G. Wilson, M. C. Stefan, X. Zhou, P. C. Dastoor, W. J. Belcher, Sol. Energ. Mat. Sol. C **128**, 369 (2014).
[13] M. Maute, S. Raible, F. E. Prins, D. P. Kern, H. Ulmer, U. Weimar, W. Göpel, Sens. Actuators B **58**, 505 (1999).
[14] C. H. A. Esteves, B.A. Iglesias, R. W. C. Lia, T. Ogawa, K. Araki, J. Gruber, Sens. Actuators B **193**, 136 (2014).
[15] L. O. Péres, R. W. C. Li, E. Y. Yamauchi, R. Lippi, J. Gruber, Food Chem. **130**, 1105 (2012).
[16] X. B. Ren, H.X. Huang, M. Chen, D. J. Qian, Synthetic Met. **167**, 10 (2013).
[17] Z. Ozbek, M. Erdogan, R. Capan, Sens. Actuators B **196**, 328 (2014).
[18] P. I. Chen, D. Tang, X. Wang, H. Chen, M. Liu, J. Li, X. Liu, Colloid Surface A **175**, 171 (2000).
[19] I. Çapan, Ç. Tarımcı, M. Erdoğan, A. K. Hassan, Mat. Sci. Eng. C **29**, 1114 (2009).
[20] F. Liu, X. Liu, S. C. Ng, H. S. O. Chan, Sens. Actuators B **113**, 234 (2006).
[21] M. Ozmen. Z. Ozbek, S. Buyukcelebi, M. Bayrakci, S. Ertul, M. Ersoz, R. Capan, Sens. Actuators B **190**, 502 (2014).
[22] M. Ozmen, Z. Ozbek, M. Bayrakci, S. Ertul, M. Ersoz, R. Capan, Sens. Actuators B **195**, 156 (2014).
[23] M. Ozmen. Z. Ozbek, M. Bayrakci, S. Ertul, M. Ersoz, R. Capan, App. Surf. Sci. **359**, 364 (2015).
[24] A. N. Kursunlu, Y. Acikbas, M. Ozmen, M. Erdogan, R. Capan, Analyst **142**, 3689 (2017).
[25] Y. Acikbas, S. Z. Bas, M. Ozmen, R. Capan, M. Erdogan, IEEE Sen. J. **17(5)**, 1222 (2017).
[26] Y. Acikbas, R. Capan, M. Erdogan, N. Cankaya, C. Soykan, J. M. S.-Pure Appl. Chem. **53 (3)**, 132 (2016).
[27] Y. Acikbas, R. Capan, M. Erdogan, F. Yükrük, App. Surf. Sci. **350**, 135 (2015).
[28] A. K. Hassan, A. V. Nabok, A. K. Ray, A. Lucke, K. Smith, C. J. M. Stirling, F. Davis, Mater. Sci. Eng. C **8–9,** 251 (1999).
[29] M. Erdogan, R. Capan, F. Davis, Sens. Actuators, B: Chem. **145**, 66 (2010).
[30] J. Crank, The Mathematics of Diffusion, London: Oxford University Press, 1970.
[31] M. Erdogan, Z. Özbek, R. Çapan, Y. Yagci, J. Appl. Polym. Sci. **123**, 2414 (2012).
[32] M. Erdogan, I. Capan, C. Tarimci, A. K. Hassan, J. Colloid Interf. Sci. **323**, 235 (2008).
[33] O. Pekcan, N. Adiyaman, S. Ugur, J. Appl. Polym. Sci. **84**, 632 (2002).
[34] Y. Acikbas, R. Capan, M. Erdogan, L. Bulut, C. Soykan, Sens. Actuators, B: Chem. **241,** 1111 (2017).
[35] V. C. Gonçalves, D.T. Balogh, Sens. Actuators, B: Chem. **142**, 55 (2009).

*Corresponding author: yaser.acikbas@usak.edu.tr